

# Source-Driven Tails in Kerr Spacetime: Nonlinear effects in Late-Time Behavior

Som Dev Bishoyi,<sup>1, 2, \*</sup> Subir Sabharwal,<sup>3, †</sup> and Gaurav Khanna<sup>4, 5, 2, 3, ‡</sup>

<sup>1</sup>*Department of Mathematics, University of Massachusetts Dartmouth,  
285 Old Westport Rd., North Dartmouth, MA 02747, USA*

<sup>2</sup>*Center for Scientific Computing & Data-Science Research, University of Massachusetts Dartmouth,  
285 Old Westport Rd., North Dartmouth, MA 02747, USA*

<sup>3</sup>*Institute for AI & Computational Research, University of Rhode Island, Kingston, RI 02881, USA*

<sup>4</sup>*Department of Physics, University of Rhode Island, Kingston, RI 02881, USA*

<sup>5</sup>*Department of Physics, University of Massachusetts Dartmouth,  
285 Old Westport Rd., North Dartmouth, MA 02747, USA*

(Dated: January 19, 2026)

We present the long-duration time-domain simulations of scalar-field tails in Kerr spacetimes driven by *outgoing* multipolar sources. Extending the recent work in the literature from Schwarzschild to rotating black holes, we evolve sources with  $\ell' = \{0, 1, 2, 3, 4\}$  on backgrounds with dimensionless spin  $a/M = \{0.0, 0.8, 1.0\}$  and extract the late-time decay rates of measured modes  $\ell \leq 4$  for a nonlinearity-inspired outgoing source with a  $1/r^2$  fall-off. In all cases we find the inverse power-law index  $p_{\ell\ell'}$  to be larger than the source-free Price law values by one unit, i.e.  $p_{\ell\ell'}^{\text{sourced}} = p_{\ell\ell'}^{\text{Price}} + 1$ . We also include a power-law index value computation for a similar source-driven gravitational wave case  $(\ell, m) = (4, 4)$  and confirm closely related results in the recent literature.

## CONTENTS

<b>I. Introduction</b>	1
A. Motivation	1
B. Key results	2
C. Organization	2
<b>II. Background</b>	2
A. Homogeneous Teukolsky equation	2
B. Non-linearity inspired source	3
<b>III. Numerical Implementation</b>	3
A. Simulation catalog	3
B. Power-law extraction	4
<b>IV. Results</b>	4
A. Results: Sub-Extremal Kerr	4
B. Results: Extremal Limit	5
C. Results: Gravitational wave case	5
<b>V. Discussion and Conclusions</b>	5
<b>Acknowledgments</b>	6
<b>References</b>	6

## I. INTRODUCTION

### A. Motivation

The monumental detection of gravitational waves (GW) by the LIGO–Virgo–KAGRA network have promoted the ringdown phase of binary-black-hole mergers to a powerful laboratory for testing the strong-field regime of general relativity (GR) [1–4]. While the early ringdown is governed by a discrete set of quasinormal modes (QNMs) determined by the linearized Einstein equations, the signal at late retarded times is known to transition to an inverse power-law “tail” first predicted by Price half a century ago [5, 6]. These tails arise from back-scattering off the effective curvature potential surrounding the black hole and fall off as  $\Psi_\ell \propto t^{-2\ell-3}$  in Schwarzschild spacetimes when the initial data have compact support (Here  $\ell$  denotes the field multipole under study).

With the advent of third-generation ground-based observatories [7, 8] and the space-based mission LISA [9], the sensitivity to late-time ringdown will improve considerably, making it essential to understand every physical effect that can modify the traditional picture. Recent work [10, 11, 13] has demonstrated that even within GR, *non-linear* couplings at second perturbative order produce a *slower* decay for a scalar field on a Schwarzschild background. In these studies, the lowest order non-linear effects are modeled as a source-term in the linear theory and the resulting tails are computed. These tails exhibit slower decay when compared to Price tails that arise from initial data as opposed to a source. Similar conclusions were obtained independently in Ref. [14]. Because a slower tail may dominate the late-signal, non-linear effects must be quantified to avoid systematic biases in spectroscopic analyses.

\* sbishoyi@umassd.edu

† subir@uri.edu

‡ gkhanna@uri.edu

Rotating (Kerr) black holes are astrophysically generic and introduce several complications absent in the non-spinning case: (i) mode mixing between different  $\ell$  due to the spheroidal structure of Kerr QNMs; (ii) frame dragging, which modifies the effective potential that sources back-scattering; and (iii) an additional near-horizon, near-extremal (NHEK) region where perturbations can linger, affecting the late-time field seen by distant observers [15–18]. Although linear tails in Kerr have been studied extensively both analytically and numerically [19–24, 26, 27], the non-linear problem remains largely unexplored. The generalization of Price law to sub-extremal Kerr spacetimes for the case of compact initial data located with no support on the horizon is given by [23, 26, 27]<sup>1</sup>:

$$p_{\ell\ell'} = \begin{cases} -(\ell' + \ell + 3) & \text{for } \ell' = 0, 1 \\ -(\ell' + \ell + 1) & \text{otherwise} \end{cases} \quad (1)$$

along  $r = \text{const}$  and at  $\mathcal{H}^+$ , and

$$p_{\ell\ell'}^{\mathcal{I}^+} = \begin{cases} -\ell' & \text{for } \ell \leq \ell' - 2 \\ -(\ell + 2) & \text{for } \ell \geq \ell' \end{cases} \quad (2)$$

along null infinity  $\mathcal{I}^+$ , where  $\ell'$  refers to the initial field multipole, and  $\ell$  is the multipole being observed. These rates refer to axisymmetric multipoles, and were obtained by carefully studying the inter-mode coupling effects that are present in the Kerr spacetime due to the lack of spherical symmetry. The non-axisymmetric results do not change, except for fact that both  $\ell'$  and  $\ell$  are bounded from below by the value of  $m$  [28]. The extremal case has a similar behavior with the exception that the horizon rates match the null infinity rates due to the presence of a conformal symmetry [34].

The primary aim of this work is therefore to *numerically* generalize the findings of Refs. [10–12] to Kerr spacetimes and to map out the dependence of the late-time power-law index  $p_{\ell\ell'}$  on both the source multipole  $\ell'$  and the observed  $\ell$  mode and zero initial data. We focus on scalar fields as a computationally economical proxy for the gravitational case. However, we also include a result for the lowest-order non-linear effect in the gravitational wave case. Our study is the first to perform evolutions of non-linearity inspired, source-driven simulations of mode-coupled scalar tails for long simulation times  $t/M, u/M \gtrsim 10^3$  using a modern GPU-accelerated WENO code. The results serve as a crucial stepping stone toward full gravitational-wave predictions and have direct implications for template accuracy in upcoming high-signal-to-noise detections.

## B. Key results

Our main findings for the case of Kerr tails driven by a nonlinearity-inspired source with multipole  $\ell'$  appear below:

1. For all spins (including extremal) the numerical power-law tails match the general prediction of Ref. [10] for both  $r = \text{const}$  timelike worldline and along null infinity  $\mathcal{I}^+$ . More specifically, the power-law follows the values in Eqns. 1 and 2 simply increased by one unit.
2. As argued by Ref. [10, 11] the lowest order effect of nonlinearities should appear in the  $\ell = m = 4$  gravitational wave mode from the squared  $\ell' = m' = 2$  mode acting as the source. Our results agree with Ref. [10] i.e.,  $t^{-10}$  on a  $r = \text{const}$  time-like worldline. Note that Ref. [10] and Ref. [11] results appear to be in tension since they make different claims on the power-law index, however the difference can be reconciled since their results use different gauge choices.

In summary,

$$p_{\ell\ell'}^{\text{sourced}} = p_{\ell\ell'}^{\text{Price}} + 1 \quad (3)$$

where  $p_{\ell\ell'}^{\text{Price}}$  refers the well-known Price law and its generalization to Kerr spacetime with no source and initial data  $\ell'$  as given in Eqns. 1 and 2. Recall that the meaning of  $\ell'$  is different in the different terms of Eqn. 3. On the left-hand-side of the equation,  $\ell'$  labels the multipole value of the source term, whereas on the right-hand-side it is the multipole value of the initial data.

## C. Organization

Section II reviews linear and non-linear tail theory in Kerr. Section III details our numerical implementation, including the evolution scheme, boundary conditions, parallelization strategy, and code-validation tests. Section IV A presents our power-law index extractions, and a comprehensive set of tables for  $\ell', \ell \leq 4$  across a sub-extremal spin value. The extremal limit is treated separately in Sec. IV B. We conclude in Sec. V with an outlook toward future calculations and observable consequences.

## II. BACKGROUND

In this section, we briefly describe the Teukolsky equation and the coordinate systems used to derive the evolution equations that are solved numerically. We also describe how an outgoing pulse whose amplitude falls off radially can be used as a model for a source term inspired from non-linearities.

---

<sup>1</sup> Sometimes referred to as the “ZKB formula” since it was first presented in Ref. [23].

### A. Homogeneous Teukolsky equation

We consider perturbations  $\Psi(t, r, \theta, \phi)$  propagating on a fixed Kerr geometry of mass  $M$  and angular momentum  $J = aM$ . The dynamics of scalar, vector and tensor field perturbations in the spacetime of Kerr black holes is governed by the Teukolsky equation:

$$\begin{aligned} & - \left[ \frac{(r^2 + a^2)^2}{\Delta} - a^2 \sin^2 \theta \right] \partial_{tt} \Psi - \frac{4Mar}{\Delta} \partial_{t\phi} \Psi \\ & - 2s \left[ r - \frac{M(r^2 - a^2)}{\Delta} + ia \cos \theta \right] \partial_t \Psi \\ & + \Delta^{-s} \partial_r (\Delta^{s+1} \partial_r \Psi) + \frac{1}{\sin \theta} \partial_\theta (\sin \theta \partial_\theta \Psi) + \\ & \left[ \frac{1}{\sin^2 \theta} - \frac{a^2}{\Delta} \right] \partial_{\phi\phi} \Psi + 2s \left[ \frac{a(r - M)}{\Delta} + \frac{i \cos \theta}{\sin^2 \theta} \right] \partial_\phi \Psi \\ & - (s^2 \cot^2 \theta - s) \Psi = 0, \end{aligned} \quad (4)$$

where  $M$  is the mass of the Kerr black hole,  $a$  its angular momentum per unit mass,  $\Delta = r^2 - 2Mr + a^2$ . The  $s = 0$  version of this equation describes scalar fields. When  $s = -2$  the Teukolsky master variable describes outgoing gravitational radiation and is related to the perturbed Weyl Scalar  $\Psi_4$  by  $\Psi = \rho^{-4} \Psi_4$  where  $\rho = -1/(r - ia \cos \theta)$ . Unless stated otherwise, we use  $\Psi$  to denote the first-order perturbation  $\Psi^{(1)}$  about the background value, in accordance with standard practice in the literature.

Due to the presence of coordinate singularities in the metric at  $\Delta = 0$ , we switch to a better suited coordinate system known as ingoing Kerr coordinates. These coordinates are able to smoothly penetrate the horizon of a black hole. These new coordinates  $(\tilde{t}, r, \theta, \tilde{\phi})$  are related to the Boyer-Lindquist coordinates by

$$\tilde{\phi} = \phi + \int \frac{a}{\Delta} dr \quad (5)$$

$$\tilde{t} = t - r + r_* \quad (6)$$

where the tortoise radial coordinate  $r_* = \int (r^2 + a^2) \Delta^{-1} dr$ . At late times, the  $\tilde{t}$  variable essentially becomes the null variable  $v = t + r_*$  at the horizon. The next step that goes into the setup of our coordinate system is hyperboloidal compactification as developed by Zenginoğlu [29]. To do this, we define a compactified coordinate system  $(\tau, \rho, \theta, \varphi)$  by

$$\tau = \tilde{t} - r^2/(r + S) + 4 \ln[S/(r + S)] \quad (7)$$

and

$$\rho = r/[1 + r/S] \quad (8)$$

where a free parameter  $S$  controls both the domain and also the foliation. Note that  $\rho \in [0, S]$  maps  $r \in [0, \infty)$  and is therefore a one-to-one compactifying coordinate.

A Penrose diagram of the slices defined by these coordinates in the Kerr spacetime context can be found in Ref. [29]. We do not show the final form of the equation in these compactified coordinates because of the lengthy nature of the expression and the fact that it is not particularly illuminating. In symbolic form, it can be written as

$$\begin{aligned} & A^{\tau\tau} \partial_\tau^2 \psi + A^{\tau\rho} \partial_\tau \partial_\rho \psi + A^{\rho\rho} \partial_\rho^2 \psi + A^{\theta\theta} \partial_\theta^2 \psi \\ & + B^\tau \partial_\tau \psi + B^\rho \partial_\rho \psi + B^\theta \partial_\theta \psi + C\psi = 0, \end{aligned} \quad (9)$$

Additional details on writing Eq. (9) in first-order form and the particular choice of auxiliary variables used can be found in [30].

### B. Non-linearity inspired source

To understand the behavior of non-linear effects in perturbation theory, we consider the second order quantity in the perturbative expansion of the unperturbed scalar  $\Psi$ , which we write as  $\Psi^{(2)}$ . Campanelli and Lousto first showed that the evolution of  $\Psi^{(2)}$  is also governed by the Teukolsky equation, with a source term that depends on all components of the first order metric perturbation  $h_{\mu\nu}$  [36]. The equation of motion for  $\Psi^{(2)}$  is

$$\mathcal{T}\Psi^{(2)} = \mathcal{S}[h_{\mu\nu}^{(1)}] \quad (10)$$

where  $\mathcal{T}$  is the Teukolsky operator and  $\mathcal{S}$  is the source term which depends on the first order metric perturbation  $h_{\mu\nu}^{(1)}$ .

Asymptotic behavior of source terms in the second-order Teukolsky equation decay as  $\mathcal{O}(1)/r^2$  at infinity (See Sec. 5 in [35]). This source term can be written as

$$\mathcal{S}[h_{\mu\nu}^{(1)}] = \frac{F(u, \theta, \phi)}{r^2} + \mathcal{O}(r^{-3}) \quad (11)$$

where  $u = t - r_*$  is the retarded time coordinate. As a simpler and computationally light-weight approximation, we choose a Gaussian source moving radially outward with the appropriate falloff to model an outgoing first-order perturbation. The resulting non-linearity inspired source becomes

$$\mathcal{S}(u, \theta, \phi) \sim \frac{G(u - u_0)}{r^2} Y_{\ell'm'}(\theta, \phi) \quad (12)$$

where  $G$  is a standard Gaussian function.

### III. NUMERICAL IMPLEMENTATION

Our numerical implementation scheme entails re-writing the second order partial differential equation (PDE) above in terms of two coupled first-order differential equations. We solve this system using a high-order weighted essentially non-oscillatory (WENO) finite-difference scheme with explicit Shu-Osher time-stepping.

Details may be found in our previous work [30]. In the Schwarzschild case, we set  $S = 18.0$ , while in the Kerr cases we choose  $S = 18.4$  for  $a/M = 0.8$  and  $S = 19.0$  for  $a/M = 1.0$ . The source is a Gaussian of unit width in  $u$  with a radial fall-off of  $1/r^2$  which essentially is the  $\beta = 2$  case in Ref. [10]. The initial data is set to zero, so we only obtain outgoing source-driven tails in this work and not those driven by initial data. The angular distribution of the source is characterized by the  $\ell'$  multipole. We use high-precision floating-point arithmetic, so that we can track decaying values for long durations accurately. Specifically, we use 128-bit quadruple-precision, which is particularly important for accurately studying the  $\ell = 4$  multipole mode.

Finally, to complete these long duration, high-accuracy and high-precision computations in a reasonable time-frame we make extensive use GPGPU-based parallel computing. For additional details on implementation of such intensive computations on a parallel GPU architecture, we refer the reader to our earlier work on the subject [30]. Note that these simulations take significant computational resources to run. For this reason, we focused our efforts on a single value of  $a/M$  for the sub-extremal ( $0 < a/M < 1$ ) case.

### A. Simulation catalog

We carried out  $3 \times 5 = 15$  primary simulations covering source  $\ell' = \{0, 1, 2, 3, 4\}$  and spins  $a/M = \{0.0, 0.8, 1.0\}$ . Typical resolution used was  $(N_\rho, N_\theta) = (32000, \pi/128)$  with a Courant factor of 0.64. Each computation took approximately a day on an Nvidia V100 GPU with an IBM POWER9 host.

It is worth repeating here that the evolutions include a nonlinearity-inspired source with multipole  $\ell'$  and zero initial data. This is different from the classic Price law cases wherein the initial data has a multipole  $\ell'$  and there is no source.

### B. Power-law extraction

For each  $(\ell', \ell)$  we compute the instantaneous log-slope (so-called “LPI” for local power-law index). For example, at null infinity this quantity takes the form

$$p_{\ell\ell'}(u) = \frac{d \ln |\Psi_\ell|}{d \ln u}, \quad (13)$$

and is computed using a centered 4-point finite-difference stencil in  $\ln u$ . We then fit  $p_{\ell\ell'}(u)$  over the last few  $100M$  to a constant plus a term  $\propto u^{-1}$ , consistent with theoretical expectations for the next-to-leading order tail. The extrapolated constant is quoted as the power-law index; statistical fit uncertainties and the PDE solver truncation error dominate the error budget.

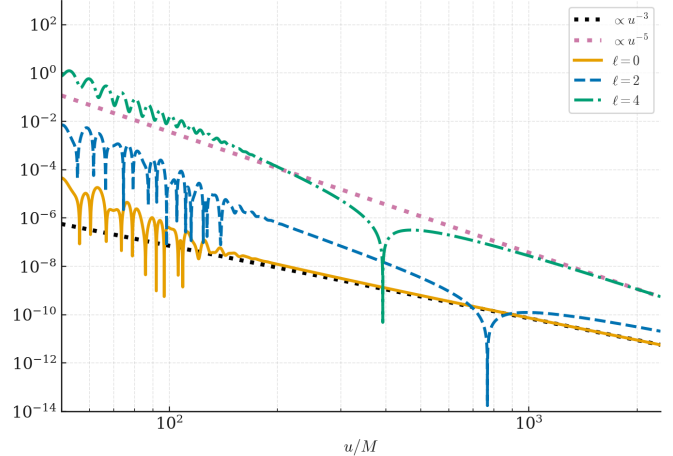


FIG. 1. Log-log plot of different angular projections  $\ell = 0, 2, 4$  of the scalar field  $\Psi^{(2)}$  vs.  $u$  at  $\mathcal{I}^+$  for  $\ell' = 4$  source for a Kerr black hole with  $a/M = 0.8$ .

## IV. RESULTS

### A. Results: Sub-Extremal Kerr

Figure 1 shows the late-time decay of  $\Psi^{(2)}$  sourced by  $\ell' = 4$  on a background with  $a/M = 0.8$ . The slopes converge to  $\{-3, -3, -5\}$  for  $\ell = \{0, 2, 4\}$  in agreement with Eqn. 3. Similar behavior occurs for all other mode pairings. Tables I-II list the extracted for each spin. The Schwarzschild results are in clear agreement with Ref. [10]. For all spinning cases the numerical power-law tails match the general prediction of Ref. [10] for both  $r = \text{const}$  timelike worldline and along null infinity  $\mathcal{I}^+$  in the sense that the power-law follows the values in Eqns. 1 and 2, simply increased by one unit.

These results are somewhat counterintuitive. One may reason that with a  $\ell'$  source, a  $\ell = \ell'$  mode would develop that would behave just as in Schwarzschild spacetime [10]. Additionally, through mode-coupling in Kerr, infinitely many  $\ell \neq \ell'$  modes would get “excited” [26]. Now, these modes are not source-driven since the source-term is non-zero only for the  $\ell'$  case. Therefore, it is reasonable to argue that those  $\ell \neq \ell'$  modes would evolve just as they do in the source-free cases, i.e. simply follow Price law

TABLE I. Inverse-power indices  $-p_{\ell\ell'}$  for Schwarzschild ( $a = 0$ ) at the locations:  $r = \text{const.}$  and  $\mathcal{I}^+$ .

$\ell'$	0	1	2	3	4
0	1.999, 1.004	—	—	—	—
1	—	4.048, 2.014	—	—	—
2	—	—	5.989, 3.087	—	—
3	—	—	—	7.983, 3.999	—
4	—	—	—	—	9.813, 5.042

in Kerr as in Eqns. 1 and 2. However, that is *not* what we observe at all. Our results show that *all*  $\ell$  modes follow Eqn. 3 and decay slower than what one may have argued through intuitive reasoning. Further investigation is needed to fully understand this rather intriguing result.

## B. Results: Extremal Limit

We can take  $a = M$  using our numerical approach and study the late-time behavior of the scalar field multipoles. Table III presents the results. One expects the  $r = \text{const}$  and null infinity  $\mathcal{I}^+$  tails to behave the same as the sub-extremal case, however the horizon tails would be different. For this reason we present the horizon and  $\mathcal{I}^+$  rates only. It is interesting to note that the horizon rates here do not appear to match the null infinity rates as one may expect due to the conformal symmetry [34] in extremal spacetimes. In fact, they appear to simply match the source-free, initial data driven results, i.e. follow the Price law equivalent for extremal Kerr [33]. We speculate that it is due to a breakdown of this conformal symmetry between  $\mathcal{H}^+$  and  $\mathcal{I}^+$  because of the presence of an outgoing source-term. Further investigation is needed to fully understand this result.

It is worth noting that the type of source [10] we have studied in this work does not have any impact on the Aretakis charge values on the horizon. Additionally, as shown in [10] only an *outgoing* source changes the power-law decay rates from Price tails, thus minimizing an opportunity for the source to leave any footprint on the horizon. Thus, the Aretakis charges will continue to arise through the imposition of non-trivial initial data on the horizon – a case that we have studied elsewhere [33] and not in this work.

## C. Results: Gravitational wave case

Now we turn to the lowest-order gravitational case with non-linear effects that has received some attention in the recent literature.

As argued in Ref. [10, 11] the lowest order effect of nonlinearities should appear in the  $\ell = m = 4$  gravitational wave mode of  $\Psi^{(2)}$  from the squared  $\ell' = m' = 2$  mode of  $\Psi^{(1)}$  as source. Ref. [10] results suggest that the  $r =$

TABLE II. Inverse-power indices  $-p_{\ell\ell'}$  for Kerr ( $a = 0.8$ ) at the locations:  $r = \text{const.}$  and  $\mathcal{I}^+$ .

$\ell'$	$\ell$				
	0	1	2	3	4
0	1.998, 1.003	–	3.994, 2.993	–	6.110, 4.800
1	–	4.050, 2.011	–	5.992, 4.011	–
2	2.001, 1.008	–	3.901, 2.997	–	6.210, 5.010
3	–	3.998, 2.020	–	6.020, 3.952	–
4	3.920, 3.036	–	6.206, 2.861	–	7.752, 4.820

TABLE III. Inverse-power indices  $-p_{\ell\ell'}$  for the extremal Kerr at the locations:  $\mathcal{H}^+$  and  $\mathcal{I}^+$ .

$\ell'$	$\ell$				
	0	1	2	3	4
0	2.005, 0.993	–	4.009, 3.005	–	6.034, 5.008
1	–	3.002, 2.000	–	4.970, 4.035	–
2	1.895, 1.022	–	3.970, 3.020	–	5.919, 5.018
3	–	2.992, 2.007	–	4.980, 4.199	–
4	3.854, 3.047	–	3.920, 2.998	–	6.161, 4.822

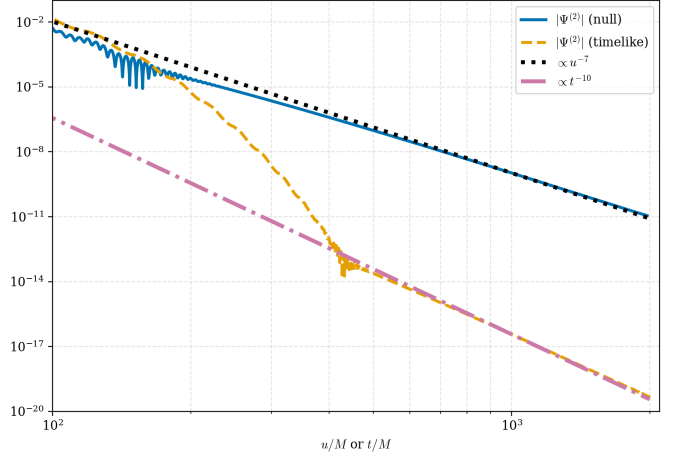


FIG. 2. Log–log plot of the  $(\ell, m) = (4, 4)$  angular projection of  $|\Psi^{(2)}|$  vs.  $t, u$  with  $(\ell', m') = (2, 2)$  squared source and  $a/M = 0.8$ .

const rates should be  $t^{-10}$ , while the Price tails formula would suggest a tail of  $t^{-11}$ .

Our results depicted in Fig. 2 confirm those results i.e.  $t^{-10}$  on a  $r = \text{const}$  timelike worldline for  $|\Psi^{(2)}|$ . At  $\mathcal{I}^+$  we obtain a late-time behavior of  $u^{-7}$  which is one power slower than the source-free case [25]. Our results have been consistent throughout in the general sense that the rates with the nonlinearity-inspired source decay slower than Price law by a single power.

## V. DISCUSSION AND CONCLUSIONS

In this work we evolve scalar fields with outgoing sources with  $\ell' = \{0, 1, 2, 3, 4\}$  on black hole backgrounds with dimensionless spin  $a/M = \{0.0, 0.8, 1.0\}$  and extract the late-time decay rates of measured modes  $\ell \leq 4$ . In all cases we find the inverse power-law index to be larger than the source-free Price law values by one unit, i.e.  $p_{\ell\ell'}^{\text{sourced}} = p_{\ell\ell'}^{\text{Price}} + 1$ . This result is counterintuitive given the common understanding of mode-coupling in Kerr spacetime. More specifically, given that the source is only non-zero for multipole  $\ell'$ , one would expect the tails for the  $\ell \neq \ell'$  cases to not change.

We also study a power-law index value for the gravitational wave case  $(\ell, m) = (4, 4)$  driven by a  $(\ell', m') =$

(2, 2) squared source, and confirm related results in the recent literature.

The form of the outgoing source is inspired by the lowest order nonlinearity that is envisioned to appear in second-order perturbation theory. Our results are interesting because they suggest that with the inclusion of non-linearity, the tails decay slower and that may increase their chances of being observed by the next generation of gravitational wave observatories. In fact, early full numerical relativity simulations [14] offer some compelling evidence that indeed, the power-law decays are much slower than those predicted by Price law.

Future natural extensions of this work would be in two directions: (i) more extensive study of the gravitational wave case, and (ii) a broader study of the nonlinear terms that may impact the expected outcomes from linear theory.

To conclude, the late-time behavior of a perturbed

Kerr black hole is more intricate than linear theory foretold, yet its leading imprint can still be captured by a remarkably simple power law. We hope the present work paves the way for a comprehensive, nonlinear understanding of black-hole ringdown in the era of precision gravitational-wave astronomy.

## ACKNOWLEDGMENTS

G.K. acknowledges support from NSF Grants No. PHY-2307236 and DMS-2309609. S.B. acknowledges support of NSF grants PHY-2110496 and DMS-2309609. All computations were performed on the UMass-URI UNITY HPC/AI cluster at the Massachusetts Green High-Performance Computing Center (MGHPCC). We also acknowledge the use of OpenAI's ChatGPT for assistance with summarizing some background material in an initial draft.

---

[1] B. P. Abbott *et al.* (LIGO Scientific Collaboration and Virgo Collaboration), “Observation of Gravitational Waves from a Binary Black Hole Merger,” *Phys. Rev. Lett.* **116**, 061102 (2016).

[2] E. Berti *et al.*, “Testing General Relativity with Present and Future Astrophysical Observations,” *Class. Quant. Grav.* **32**, 243001 (2015).

[3] E. Berti *et al.*, “Black hole spectroscopy: from theory to experiment,” arXiv:2505.23895 (2025).

[4] N. Yunes *et al.*, “Gravitational-wave tests of general relativity with ground-based detectors and pulsar-timing arrays,” *Living Rev. Relativity* **28**, 3 (2025).

[5] R. H. Price, “Nonspherical perturbations of relativistic gravitational collapse. I. Scalar and gravitational perturbations,” *Phys. Rev. D* **5**, 2419 (1972).

[6] R. H. Price, “Nonspherical perturbations of relativistic gravitational collapse. II. Integer-spin, zero-rest-mass fields,” *Phys. Rev. D* **5**, 2439 (1972).

[7] M. Maggiore *et al.*, “Science Case for the Einstein Telescope,” *JCAP* **03** (2020) 050.

[8] D. Reitze *et al.*, “Cosmic Explorer: The U.S. Contribution to Gravitational-Wave Astronomy beyond LIGO,” *Bull. Am. Astron. Soc.* **51**, 035 (2019).

[9] P. Amaro-Seoane *et al.* (LISA Consortium), “Laser Interferometer Space Antenna,” arXiv:1702.00786 (2017).

[10] V. Cardoso *et al.*, “Hushing black holes: Tails in dynamical spacetimes,” *Phys. Rev. D* **109**, L121502 (2024).

[11] A. Kehagias and A. Riotto, “Nonlinear Tails of Gravitational Waves in Schwarzschild Black Hole Ringdown,” arXiv:2503.06224 (2025).

[12] D. Gajic and L. Kehrberger, “Linear and nonlinear late-time tails on dynamical black hole spacetimes via time integrals,” arXiv:2511.23242 (2025).

[13] S. Ling, S. Shah and S. C. Wong, “Dynamical nonlinear tails in Schwarzschild black hole ringdown,” arXiv:2503.19967 (2025).

[14] M. DeAmicis *et al.*, “Late-time tails in nonlinear evolutions of merging black holes,” arXiv:2412.06887 (2024).

[15] L. M. Burko, G. Khanna, “Gravitational waves from a plunge into a nearly extremal Kerr black hole,” *Phys. Rev. D* **94**, 084049 (2016).

[16] N. E. M. Rifat, G. Khanna, L. M. Burko, “Repeated ringing of black holes: Quasinormal bursts from highly eccentric, extreme mass-ratio binaries,” *Phys. Rev. Research* **1**, 033150 (2019).

[17] S. E. Gralla, S. A. Hughes, N. Warburton, “Inspiral into Gargantua,” *Class. Quant. Grav.* **33**, 155002 (2016).

[18] S. Bishoyi, S. Sabhawal, G. Khanna, “Numerical Evidence for Non-Axisymmetric Gravitational Hair for Extremal Kerr Black Hole Spacetimes with Hyperboloidal Foliations,” *Class. Quant. Grav.* **33**, 155002 (2016).

[19] M. Tiglio, L. E. Kidder and S. A. Teukolsky, “High accuracy simulations of Kerr tails: Coordinate dependence and higher multipoles,” *Class. Quant. Grav.* **25**, 105022 (2008).

[20] R. J. Gleiser, R. H. Price and J. Pullin, “Late time tails in the Kerr spacetime,” *Class. Quant. Grav.* **25**, 072001 (2008).

[21] A. Zenginoglu and M. Tiglio, “Spacelike matching to null infinity,” *Phys. Rev. D* **80**, 024044 (2009).

[22] L. M. Burko and G. Khanna, “Late-time Kerr tails revisited,” *Class. Quant. Grav.* **26**, 015014 (2009).

[23] A. Zenginoglu, G. Khanna and L. M. Burko, “Intermediate behavior of Kerr tails,” *Gen. Rel. Grav.* **46**, 1672 (2014).

[24] I. Racz and G. Z. Toth, “Numerical investigation of the late-time Kerr tails,” *Class. Quant. Grav.* **28**, 195003 (2011).

[25] K. Csukás, I. Racz and G. Z. Toth, “Numerical investigation of the dynamics of linear spin  $s$  fields on a Kerr background: Late-time tails of spin  $s = \pm 1, \pm 2$  fields,” *Phys. Rev. D* **100**, 104025 (2019).

[26] L. M. Burko and G. Khanna, “Mode coupling mechanism for late-time Kerr tails,” *Phys. Rev. D* **89**, 044037 (2014).

[27] Y. Angelopoulos, S. Aretakis and D. Gajic, “Late-time tails and mode coupling of linear waves on Kerr space-

times,” *Adv. Math.* **417**, 108939 (2023).

[28] L. M. Burko and G. Khanna, “Late-time Kerr tails: Generic and non-generic initial data sets, ‘up’ modes, and superposition,” *Class. Quant. Grav.* **28**, 025012 (2011).

[29] L. M. Burko, G. Khanna and Anil Zenginoglu, “Cauchy-horizon singularity inside perturbed Kerr black holes,” *Phys. Rev. D* **93**, 041501(R) (2016).

[30] S. E. Field, S. Gottlieb, Z. J. Grant, L. F. Isherwood and G. Khanna, “A GPU-Accelerated Mixed-Precision WENO Method for Extremal Black Hole and Gravitational Wave Physics Computations,” *Commun. Appl. Math. Comput.* **5**, 97–115 (2023).

[31] C.-W. Shu, “High order weighted essentially nonoscillatory schemes for convection dominated problems,” *SIAM Rev.* **51**, 82 (2009).

[32] S. Aretakis, “Stability and Instability of Extreme Reissner–Nordström Black Hole Spacetimes for Linear Scalar Perturbations I,” *Comm. Math. Phys.* **307**, 17 (2011).

[33] L. Burko, G. Khanna and S. Sabharwal, “Aretakis hair for extreme Kerr black holes with axisymmetric scalar perturbations,” *Phys. Rev. D* **107**, 124023 (2023).

[34] P. Bizo, H. Friedrich, “A remark about wave equations on the extreme Reissner–Nordström black hole exterior,” *Class. Quantum Grav.* **30**, 065001 (2013).

[35] A. Spiers, A. Pound and J. Moxon, “Second-order Teukolsky formalism in Kerr spacetime: Formulation and nonlinear source,” *Phys. Rev. D* **108**, no.6, 064002 (2023).

[36] M. Campanelli and C. O. Lousto, “Second order gauge invariant gravitational perturbations of a Kerr black hole,” *Phys. Rev. D* **59**, 124022 (1999).